RSC Advances

ROYAL SOCIETY OF CHEMISTRY

www.rsc.org/advances

RSC Advances

Dynamic Article Links ►

Cite this: DOI: 10.1039/c5ra00000x

www.rsc.org/RSC Advances

ARTICLE

Syntheses, Structures, Topologies, and Luminescence Properties of Four Coordination Polymers Based on Bifunctional 6-(4-pyridyl)-terephthalic Acid and Bis(imidazole) Bridging Linkers

Liming Fan,[a,b] Weiliu Fan,[a] Bin Li,[b] Xinzheng Liu,[b] Xian Zhao*[a] and Xiutang Zhang*[a,b]

Received (in XXX, XXX) Xth XXXXXXXXX 2015, Accepted Xth XXXXXXXXX 2015
DOI: 10.1039/c5ra00000x

ABSTRACT: Four mixed-ligand coordination networks, namely, $\{[Cu(pta)(1,4\text{-bimb})_{0.5}(H_2O)_{0.5}]\cdot H_2O\}_n$ (**1**), $\{[Co(pta)(4,4'\text{-bimbp})(H_2O)]\cdot H_2O\}_n$ (**2**), $\{[Cd(pta)(1,4\text{-bidb})_{0.5}]\cdot 2H_2O\}_n$ (**3**), and $\{[Zn(pta)(1,3\text{-bimb})_{0.5}]\cdot 1.5H_2O\}_n$ (**4**), were obtained under the solvothermal reactions in the presence of bis(imidazole) linkers (H_2pta = 6-(4-pyridyl)-terephthalic acid, 1,4-bidb = 1,4-bis(imidazol-1-yl)-2,5-dimethyl benzene, 1,3-bimb = 1,3-bis(imidazol-1-ylmethyl)benzene, 1,4-bimb = 1,4-bis(imidazol-1-ylmethyl)benzene, and 4,4'-bimbp = 4,4'-bis(imidazol-1-ylmethyl)biphenyl). Their structures were determined by single-crystal X-ray diffraction analyses and further characterized by elemental analyses, IR spectra, powder X-ray diffraction (PXRD), and thermogravimetric (TG) analyses. Complex **1** dispalys a novel (3,4,4)-connected topology with the Schläfli Symbol of $(4.8^2)_2(4^2.8^2.10^2)(8.10^4.12)$. Complex **2** features a 2D (3,5)-connected $(4^2.6^7.8)(4^2.6)$-**3,5L2** sheet. Complexes **3** and **4** are both exhibits 3-fold 3D→3D parallel entangled (3,4)-connected net with the Schläfli Symbols of $(4.6.8)(4.6^2.6^3)$-**fsc-3,4-C2/c** and $(4.6.8)(4.6^2.8^3)$-**3,4T1** for **3** and **4**, respectively. Moreover, the solid state luminescence and the luminescent lifetime of **3** and **4** have been investiged.

Introduction

The coordination polymers (CPs), an emerging class of functional crystalline materials, have attracted much attention for their fascinating structures, intersting topologies, as well as their potential applications in gas storage and seperation, magnetism, fluorescent, sensing, drug delivery, catalysis, and electronic devices.[1-3] Although many CPs have been construted from the assembly of metal centres and organic linkers, the prediction of such materials is still a huge challenge due to the complicated influence factors, two primary categories of which are the nature of organic linkers and the reaction conditions. [4-6]

As is known to all, the polycarboxylate ligands as well as the pyridine derivatives are two kinds of most widely used organic ligands due to their strong coordination abilities and diverse coordination modes.[7,8] Up to now, many CPs with versatile structures have been constructed from the above-mentioned two kinds of organic ligands. However, the bifunctional organic ligands, which contains carboxyl groups and pyridine ring together, are comparatively rare.[9] Generally speaking, the ligands consisting of carboxylate groups and the pyridine ring have more coordination modes to the metal ions or metal clusters and will resut in considerable structural complexity and diversity of CPs.[10] Besides, the advantages of the mixed-ligand synthetic strategy inspired us to introduce the bis(imidazole) bridging linkers into the reacton systerm.[11] As well as polycarboxylate linkers, (bis)imidazole bridging linkers are frequently used in the assembly process of coordination polymers acting in bridging pillars, guest molecules, or charge balance roles.[12] Moreover, the (bis)imidazole bridging linkers also play an important role in altering the coordination modes of polycarboxylate ligands.[13] The particular behaviors allow them to be promising candidates for designing frameworks with diverse topologies.

To the best of our knowledge, 6-(4-pyridyl)-terephthalic acid based CPs have never been documented up to now, although the H_2pta ligand possessing several interesting characters: (i) it has two carboxyl groups that may be completely or partially deprotonated, inducing rich coordination modes and allowing interesting structures with higher dimensionalities, (ii) it can act as a hydrogen-bond acceptor as well as donor, depending upon the degree of deprotonation, (iii) the two planars o the phenyl and pyridine ring can form different dihedral angles through the rotation of C−C single bonds, thus it may ligate metal centers in different orientations. These characters may lead to cavities, interpenetration, helical structures, and other novel motifs with unique topologies. Thus, these considerations inspired us to explore new coordination frameworks with designed 6-(4-

[a] *State Key Laboratory of Crystal Materials, Shandong University , Jinan 250100, China.*
E-mail: zhaoxian@icm.sdu.edu.cn.
[b] *Advanced Material Institute of Research, College of Chemistry and Chemical Engineering, Qilu Normal University, Jinan, 250013, China.*
E-mail: xiutangzhang@163.com.

†Electronic Supplementary Information (ESI) available: IR spectrum, Powder XRD patterns, TG curves and X-ray crystallographic data, CCDC 1031083-1031086 for **1-4**. See DOI: 10.1039/c5ra00000x.

pyridyl)-terephthalic acid (H_2pta) and different N-donor ancillary ligands under solvothermal conditions. In this paper, we reported the syntheses and characterizations of four novel coordination polymers: $\{[Cu(pta)(1,4\text{-}bimb)_{0.5}(H_2O)_{0.5}]\cdot H_2O\}_n$ (**1**), $\{[Co(pta)(4,4'\text{-}bimbp)(H_2O)]\cdot H_2O\}_n$ (**2**), $\{[Cd(pta)(1,4\text{-}bidb)_{0.5}]\cdot 2H_2O\}_n$ (**3**), and $\{[Zn(pta)(1,3\text{-}bimb)_{0.5}]\cdot 1.5H_2O\}_n$ (**4**), which exhibiting a systematic variation of architectures from (3,4,4)-connected $(4.8^2)_2(4^2.8^2.10^2)(8.10^4.12)$ architecture (**1**), 2D (3,5)-connected **3,5L2** sheet (**2**).3-fold (3,4)-connected **fsc-3,4-C2/c** net (**3**), to 3-fold (3,4)-connected **3,4T1** net (**4**) (Scheme 1). These results reveal that the bifunctional 6-(4-pyridyl)-terephthalic acid is a good candidate to construct interesting CPs. Moreover, the ancillary ligand backbones have great influence on the topology of coordination architectures and may be used as a tool to tune the degree of interpenetrations.

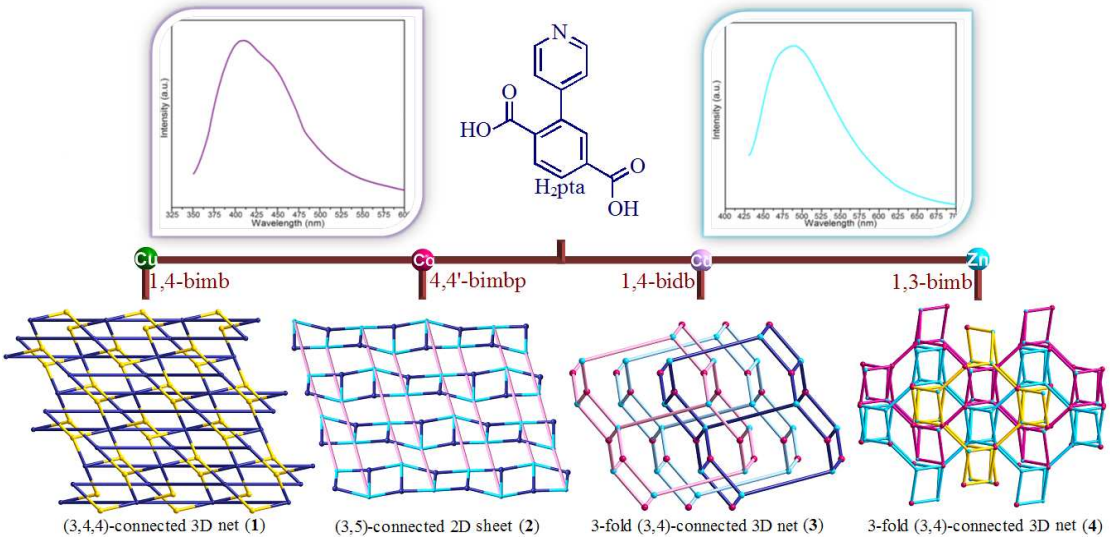

Scheme 1. Mixed-ligand strategy in the construction of complexes **1**-**4**.

Experimental Section

Materials and Physical Measurements. All chemical reagents were purchased from Jinan Henghua Sci. & Tec. Co. Ltd. without further purification. IR spectra were measured on a Nicolet 740 FTIR Spectrometer at the range of 600-4000 cm^{-1}. Elemental analyses were carried out on a CE instruments EA 1110 elemental analyzer. TGA was measured from 25 to 800 ^oC on a SDT Q600 instrument at a heating rate 5 ^oC/min under the N_2 atmosphere (100 mL/min). X-ray powder diffractions were measured on a Panalytical X-Pert pro diffractometer with Cu-Kα radiation. Fluorescence spectra were performed on a Hitachi F-4500 fluorescence spectrophotometer at room temperature. Luminscence lifetime for crystal solid samples were recorded at room temperature on an Edinburgh FLS920 phosphorimeter.

Synthesis of $\{[Cu(pta)(1,4\text{-}bimb)_{0.5}(H_2O)_{0.5}]\cdot H_2O\}_n$ (1). A mixture of H_2pta (0.20 mmol, 0.046 g), 1,4-bimb (0.20 mmol, 0.048 g), CuCl (0.20 mmol, 0.019 g), NaOH (0.40 mmol, 0.016 g), and 14 mL H_2O was placed in a Teflon-lined stainless steel vessel, heated to 170 °C for 3 days, followed by slow cooling (a descent rate of 10 ^oC/h) to room temperature. Blue block crystals of **1** were obtained. Yield of 45% (based on Cu). Anal. (%) calcd. for $C_{40}H_{34}Cu_2N_6O_{11}$: C, 53.27; H, 3.80; N, 9.32. Found: C, 52.86; H, 3.91; N, 9.23. IR (KBr pellet, cm^{-1}): 3549 (w), 3396 (m), 1619 (vs), 1580 (vs), 1538 (s), 1401 (s), 1361 (vs), 1269 (m), 846 (m), 755 (w).

Synthesis of $\{[Co(pta)(4,4'\text{-}bimbp)(H_2O)]\cdot H_2O\}_n$ (2). A mixture of H_2pta (0.20 mmol, 0.046 g), 4,4'-bimbp (0.30 mmol, 0.094 g), $Co(NO_3)_2\cdot 6H_2O$ (0.20 mmol, 0.058 g), NaOH (0.40 mmol, 0.016 g), and 12 mL H_2O was placed in a Teflon-lined stainless steel vessel, heated to 170 °C for 3 days, followed by slow cooling (a descent rate of 10 ^oC/h) to room temperature. Pink block crystals of **2** were obtained. Yield of 41% (based on Co). Anal. (%) calcd. for $C_{33}H_{28}CoN_5O_6$: C, 61.02; H, 4.35; N, 10.78. Found: C, 60.37; H, 4.63; N, 10.33. IR (KBr pellet, cm^{-1}): 3380 (m), 3125 (m), 1604 (s), 1559 (m), 1520 (s), 1368 (s), 1068 (s), 853 (m), 785 (w).

Synthesis of $\{[Cd(pta)(1,4\text{-}bidb)_{0.5}]\cdot 2H_2O\}_n$ (3). A mixture of H_2pta (0.20 mmol, 0.046 g), 1,4-bidb (0.20 mmol, 0.048 g), $CdSO_4\cdot 8/3H_2O$ (0.20 mmol, 0.051 g), NaOH (0.30 mmol, 0.012 g), and 14 mL H_2O was placed in a Teflon-lined stainless steel vessel, heated to 170 °C for 3 days, followed by slow cooling (a descent rate of 10 ^oC/h) to room temperature. Colorless block crystals of **3** were obtained. Yield of 59% (based on Cd). Anal. (%) calcd. for $C_{20}H_{18}CdN_3O_6$: C, 47.21; H, 3.57; N, 8.26. Found: C, 46.91; H, 3.47; N, 8.11. IR (KBr pellet, cm^{-1}): 3361 (m), 3111 (m), 1612 (s), 1581 (s), 1520 (vs), 1494 (vs), 1411 (s), 1373 (s), 1329 (m), 1271 (m), 849 (m),775 (w).

Synthesis of $\{[Zn(pta)(1,3\text{-}bimb)_{0.5}]\cdot 1.5H_2O\}_n$ (4). A mixture of H_2pta (0.20 mmol, 0.046 g), 1,3-bimb (0.20 mmol, 0.048 g), $ZnSO_4\cdot 7H_2O$ (0.20 mmol, 0.057 g), NaOH (0.40 mmol, 0.016 g), and 12 mL H_2O was placed in a Teflon-lined stainless steel vessel, heated to 170 °C for 3 days, followed by slow cooling (a descent rate of 10 ^oC/h) to room temperature. Colorless block crystals of **4** were obtained. Yield of 63% (based on Zn). Anal. (%) calcd. for $C_{40}H_{34}N_6O_{11}Zn_2$: C, 53.05; H, 3.78; N, 9.28. Found: C, 53.18; H, 3.74; N, 9.23. IR (KBr pellet, cm^{-1}): 3441 (s), 3114 (m), 1617 (vs), 1581 (vs), 1535 (s), 1518 (vs), 1483 (m),1401 (m), 1364 (vs), 1230 (m), 847 (m), 773 (m).

Table 1 Crystal data for **1 – 4**.

Complex	**1**	**2**	**3**	**4**
Empirical formula	$C_{40}H_{34}Cu_2N_6O_{11}$	$C_{66}H_{56}Co_2N_{10}O_{11}$	$C_{20}H_{18}CdN_3O_6$	$C_{40}H_{34}N_6O_{11}Zn_2$
Formula weight	901.81	1283.07	508.77	905.47
Crystal system	Monoclinic	Monoclinic	Monoclinic	Monoclinic
Space group	*C2/c*	*C2/c*	*C2/c*	*C2/c*
a (Å)	24.350(7)	15.0742(11)	11.979(2)	14.092(2)
b (Å)	13.403(4)	19.7770(14)	18.789(4)	18.273(3)
c (Å)	14.137(4)	21.3225(15)	18.662(5)	16.325(3)
β (°)	123.397(4)	105.1130(10)	96.494(2)	92.766(3)
V(Å^3)	3851.9(19)	6136.9(8)	4173.4(15)	4198.9(11)
Z	4	4	8	4
D_{calcd} (Mg/m^3)	1.555	1.389	1.619	1.432
μ(mm^{-1})	1.175	0.611	1.088	1.208
θ range (°)	1.82–25.00	1.74–27.10	2.03–25.00	1.83–25.00
Reflections collected	9700	15786	10389	10648
Data / restraints / parameters	3380/4/278	6681/589/485	3680/6/288	3706/4/277
F(000)	1848	2656	2040	1856
T(K)	296(2)	296(2)	296(2)	296(2)
R_{int}	0.0358	0.0386	0.0166	0.0451
R_1 (wR_2) (all data)	0.0543 (0.1070)	0.0783 (0.1780)	0.0330 (0.1156)	0.0824 (0.2218)
Gof	0.999	1.004	1.000	0.999

$R_1 = \Sigma| |F_o|-|F_c| | / \Sigma|F_o|$, $wR_2 = [\Sigma w(F_o^2-F_c^2)^2]/ \Sigma w(F_o^2)^2]^{1/2}$

X-ray crystallography. Intensity data collection was carried out on a Siemens SMART diffractometer equipped with a CCD detector using Mo-*Kα* monochromatized radiation (λ = 0.71073 Å) at 296(2) K. The absorption correction was based on multiple and symmetry-equivalent reflections in the data set using the SADABS program based on the method of Blessing. The structures were solved by direct methods and refined by full-matrix least-squares using the SHELXTL package.[14] Anisotropic thermal factors were assigned to all the non-hydrogen atoms. Hydrogen atoms were included in calculated positions and refined with isotropic thermal parameters riding on the parent atoms. And the hydrogen atoms attached to oxygen were refined with O-H=0.85Å and $U_{iso}(H) = 1.2U_{eq}(O)$. In complex **2**, the occupancy ratio of O1w is 50. Crystallographic data for complexes **1**–**4** are given in Table 1. Selected bond lengths and angles for **1**–**4** are listed in Table S1. For complexes of **1**–**4**, further details on the crystal structure investigations may be obtained from the Cambridge Crystallographic Data Centre, CCDC, 12 Union Road, CAMBRIDGE CB2 1EZ, UK, [Telephone:+44-(0)1223-762-910, Fax: +44-(0)1223-336-033; Email: deposit@ccdc.cam.ac.uk, http://www.ccdc.cam.ac.uk/deposit], on quoting the depository number CCDC-1031084 for **1**, 1031085 for **2**, 1031086 for **3**, and 1031083 for **4**.

Result and discussion

Syntheses and Characterization. Complexes **1-4** were obtained by employing bifunctional 6-(4-pyridyl)-terephthalic acid (H_2pta) and four different bis(imidazole) bridging linkers. The solid states of **1**−**4** are stable upon extended exposure to air. Powder X-ray diffraction (PXRD) has been used to check the phase purity of the bulk samples in the solid state. For complexes **1**−**4**, the measured PXRD patterns closely match the simulated patterns generated from the results of single crystal diffraction data, indicative of pure products (Fig. S1, see Supporting Information). The absorption bands of IR spectrum in the range of 3300-3500 cm^{-1} for **1-4** can be attributed to the characteristic peaks of water O-H vibrations. The absence of the expected characteristic bands around 1700 cm^{-1} is attributable to the complete deprotonation of the H_2pta ligand in the reactions. The strong antisymmetric (ν_{as}) and symmetric (ν_s) carboxyl vibrations are observed at about 1600 and 1400 cm^{-1}, respectively. And the $\Delta\nu_{as-s}$ values of 177 cm^1, 132 cm^{-1} for **1**, 206 cm^{-1}, 189 cm^{-1} for **2**, 118 cm^{-1}, 170 cm^{-1} for **3**, and 180 cm^{-1}, 171 cm^{-1} for **4**, respectively (Fig. S2).[15]

Structural Description of {[Cu(pta)(1,4-bimb)$_{0.5}$(H_2O)$_{0.5}$]·H_2O}$_n$ (1). Structural analysis reveals that complex **1** crystallizes in the monoclinic system, space group *C2/c* and the asymmetric unit contains two halves of Cu^{II} ions, one pta^{2-} ligand, half of 1,4-bimb ligand, half of coordinated water molecule, and one lattice water molecule (Fig. 1a). Cu(1) and Cu(2) show different coordination environments. Cu(1) is penta-coordinated by two N atoms from two independent pta^{2-} ligands, two carboxylate O atoms from two pta^{2-} ligands, and one coordinated water molecule. The Cu(2) ion has a distorted {CuO_2N_4} octahedral geometry, completed by four O atoms from two carboxyl groups of two pta^{2-} ligands and two N atoms from two 1,4-bimb ligands. The bond lengths of Cu−N/O are in the range of 1.961(3) −2.546(4) Å.

The pta^{2-} ligand acts as one μ_3 node to coordinate with three Cu^{II} ions *via* the deprotonated carboxylate oxygen atom and the N atom (Mode I, Scheme 2). The dihedral angle between the phenyl ring and pyridine ring in pta^{2-} is 44.53(1)°. In complex **1**, Cu(1) ions are coordinated by pta^{2-} ligands to form a 1D loop chain along *c* axis with the Cu···Cu distance being 8.052 Å. And the 1D loop chains are further expanded to a 2D (3,4)-connected [Cu(pta)]$_n$ layer by linking the Cu(2) atoms (Fig. 1b). Finally, the bridging 1,4-bimb ligands hinged the neighbouring layers together to result in a 3D [Cu(pta)(1,4-bimb)]$_n$ framework (Fig. 1c) with the 1,4-bimb separated Cu···Cu distance being 13.897 Å. On analysis of the topology, the whole structure of complex **1** can be regarded as (3,4,4)-connected architecture with the Point Schläfli Symbol of $(4.8^2)_2(4^2.8^2.10^2)(8.10^4.12)$ from the viewpoint of topology (Fig. 1d).[16]

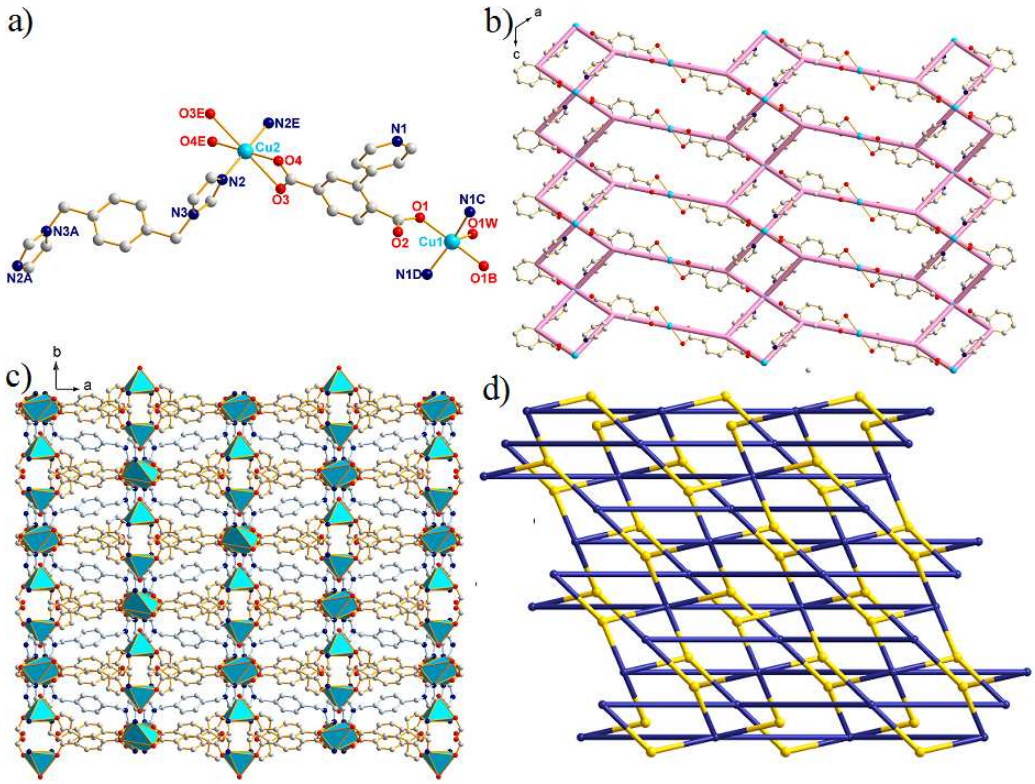

Figure 1. (a) Coordination environment of Cu^{II} ions in **1** (Symmetry codes: A: 1/2-*x*, 1/2-*y*, -*z*; B: 2-*x*, *y*, 3/2-*z*; C: 2-*x*, -*y*, 1-*z*; D: *x*, -*y*, 1/2+*z*; E: 1-*x*, -*y*, -*z*.). (b) The 3,4-connected $[Cu(pta)]_n$ sheet of **1**. (c) Schematic view of the 3D structure frameworks of **1** along *c* axis. (d) The novel (3,4,4)-connected $(4.8^2)_2(4^2.8^2.10^2)(8.10^4.12)$ architecture of **1**.

Structural Description of $\{[Co(pta)(4,4'\text{-bimbp})(H_2O)]\cdot H_2O\}_n$ (2). Structural reveals that complex **2** crystallizes in the monoclinic system, space group *C2/c*. The asymmetric unit contains two Co^{II} ions, one pta^{2-} ligand, and one 4,4'-bimbp ligand. As shown in Fig. 2a, the Co^{II} ion displays a distorted $\{CoO_3N_3\}$ octahedral geometry, completed by three N atoms from two 4,4'-bimbp ligands [Co(1)–N(2) = 2.16(17), Co(1)–N(5B) = 2.14(16) Å] and one pta^{2-} ligand [Co(1)–N(1C) = 2.20(14) Å], and three O atoms from another two pta^{2-} ligands [Co(1)–O(1A) = 2.08(12), Co(1)–O(4) = 2.11(12) Å] and one coordinated water molecule [Co(1)–O(5) = 2.16(12) Å].

Although pta^{2-} ligand also acts as one μ_3 node to coordinate with three metal ions *via* the deprotonated carboxylate oxygen atom and the N atom, it shows one different coordination mode (Mode II, Scheme 2). The dihedral angle between the phenyl ring and pyridine ring is larger than the one in **2**, 50.84(8)° in **2** and 44.53(1)° in **1**. Co ions are coordinated by pta^{2-} ligands to form a 1D wave ladder $[Co(pta)]_n$ chain, in which the adjacent three kinds of Co···Co distances being 8.756 Å, 10.230 Å, and 11.422 Å, respectively (Fig. 2b). The 4,4'-bimbp ligand adopted *cis*-coordination mode to link the Co^{II} centers together, exhibiting a 1D snake chain with the Co···Co distance being 14.637 Å. Two kinds of chains joined together by sharing the Co^{II} centers, giving a 2D layer. To illustrate the unique structure of **3**, the topological analysis approach is employed, the network of complex **2** can be rationalized to a (3,5)-connected **3,5L2** topology with the Point Schläfli symbol of $(4^2.6^7.8)(4^2.6)$ by donoting the Co^{II} ions as five-connected nodes and pta^{2-} ligands as three-connected nodes, respectively (Fig. 2c). Furthermore, neighboring layers stack in a parallel fashion along the *b* axis to form a 3D supramolecular framework with inter-layer C–H···π interactions [C(25)–H(25)···π = 3.690(1) Å, ∠C–H···π = 137.3(7)°] between the 4,4'-bimbp ligand and the phenyl ring of the pta^{2-} ligand (Fig. 2d).

Structural Description of $\{[Cd(pta)(1,4\text{-bidb})_{0.5}]\cdot 2H_2O\}_n$ (3).

The single-crystal X-ray diffraction analysis reveals that complex **3** crystallizes in the monoclinic system, space group *C2/c* space group. As shown in Fig. 3a, there is one Cd^{II} ions, one pta^{2-} ligand, one 1,4-bidb ligand, and two lattice water molecules in the asymmetric unit. Cd^{II} is hexa-coordinated, completed by four O atoms from three pta^{2-} ligands and two N atoms from one pta^{2-} ligand and one 1,4-bidb ligand, resulting in a distorted octahedral geometry. The bond lengths of Cd-O are in the range of 2.244(3)-2.488(3) Å, and the Cd-N bond lengths are 2.243(3) and 2.288(3) Å, respectively. The pta^{2-} ligand acts as one μ_3 node to coordinate with three three Cd^{II} ions by the $(\kappa^1\text{-}\kappa^1)\text{-}\mu_1$ chelating carboxyl groups and pyridyl group (Mode III, Scheme 2). The dihedral angle between phenyl ring and pyridyl ring being 49.52(0)°. Cd^{II} ions are connected by μ_3-pta^{2-} ligand to generate a 3,3-connected $[Cd(pta)]_n$ sheet (Fig. 3b). The networks are further linked by 1,4-bidb ligands to result in a 3D framework consisting of quadrilateral cavities with effective sizes of 11.63 × 13.78 $Å^2$ (Fig. 3c). Besides, the C–H···π interactions [C(20)–H(20C)···π = 2.905(9) Å, ∠C–H···π = 131.7(7)°] between the H_{methyl} and the phenyl ring of pta^{2-} in two different frameworks play important roles in maintaining the stable of final 3D interpenetrating structure.

From the topology view, complex **3** can be regard as a 3-fold 3D→3D parallel entangled (3,4)-connected **fsc-3,4-C2/c** net with Point symbol of $(4.6.8)(4.6^2.6^3)$ by denoting the Cd^{II} ions and

pta^{2-} as four- and three-connected nodes, respectively (Fig. 3d).

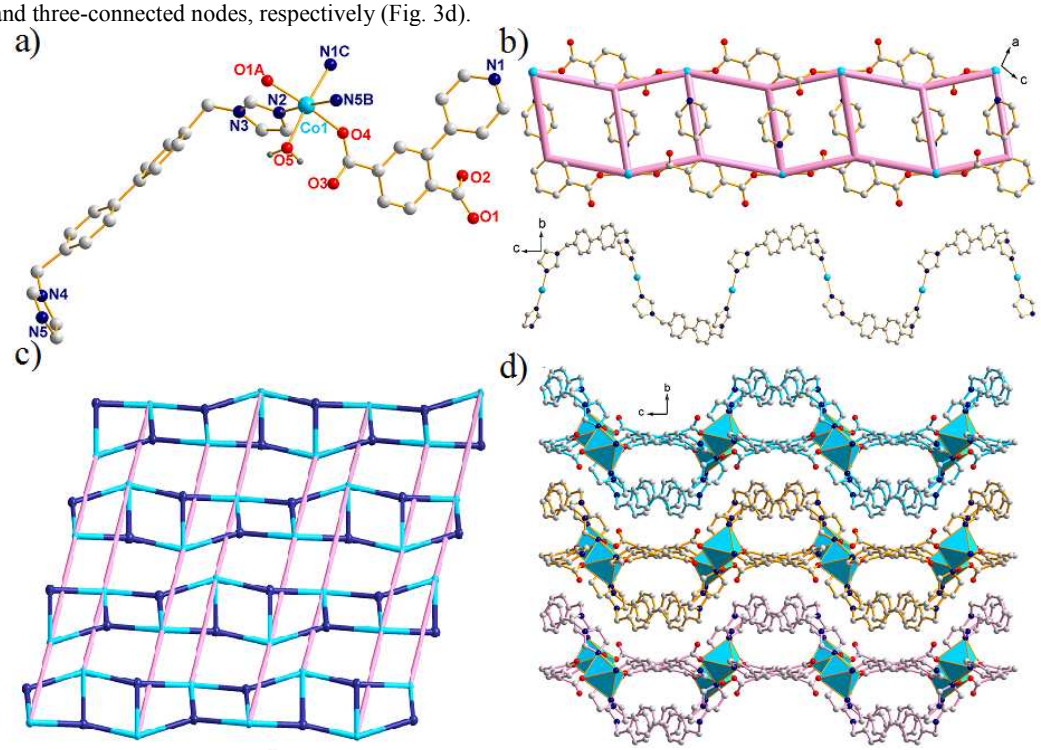

Figure 2. (a) Coordination environment of Co^{II} ion in **2** (Symmetry codes: A: –1/2+*x*, 1/2–*y*, –1/2+*z*; B: –1/2+*x*, 1/2–*y*, –1/2+*z*; C:–*x*, *y*, 3/2–*z*.). (b) The 1D $[Co(pta)]_n$ ladder chain and the 1D $[Co(4,4'\text{-bimbp})]_n$ snake chain in **2**. (c) The 2D (3,5)-connected $(4^2.6^7.8)(4^2.6)$-**3,5L2** sheet of **2**. (d) The 3D packing architecture of **2**.

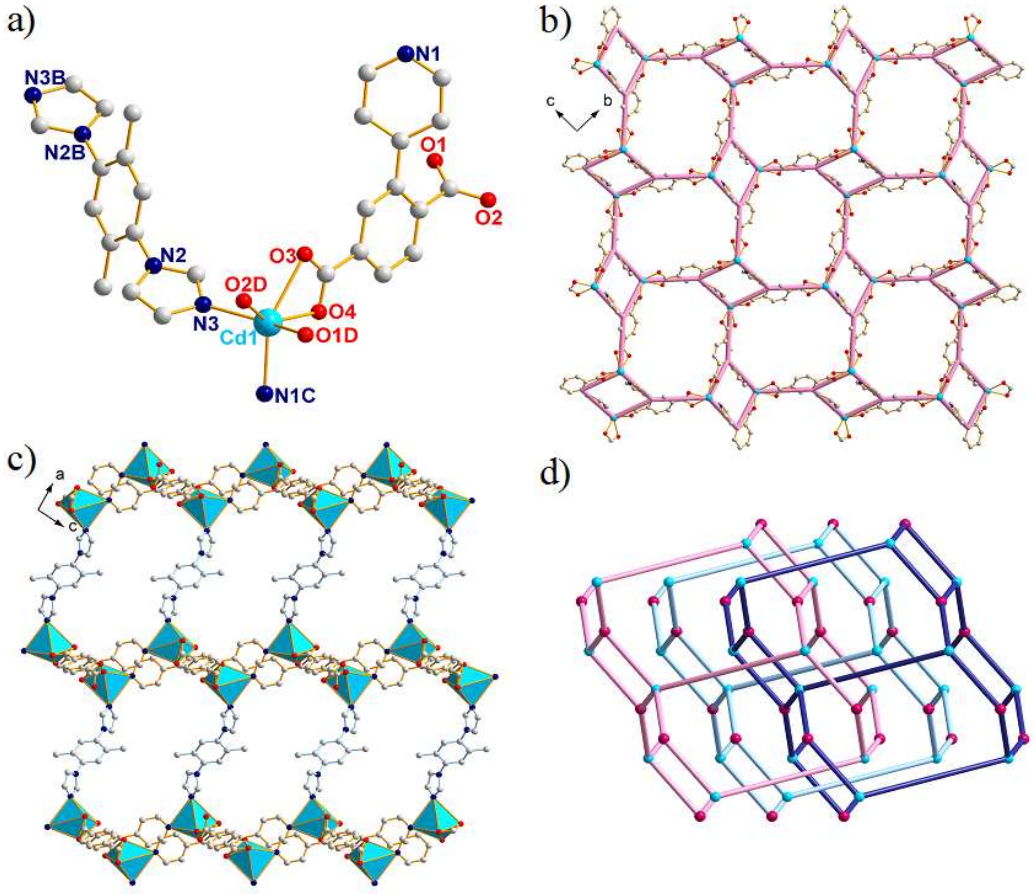

Figure 3. Coordination environment of Cd^{II} ion in **3** (Symmetry codes: B: 3/2–*x*, 1/2–*y*, -*z*; C: –1/2+*x*, 1/2–*y*, –1/2+*z*; D: 1/2–*x*, 1/2+*y*, 1/2–*z*.). (b) View of the 3,3-connected $[Cd(pta)]_n$ sheet along *a* axis. (c) Schematic view of the 3D structure frameworks of **3** along *b* axis. (d) The 3-fold 3D→3D parallel entangled (3,4)-connected $(4.6.8)(4.6^2.6^3)$-**fsc-3,4-C2/c** net.

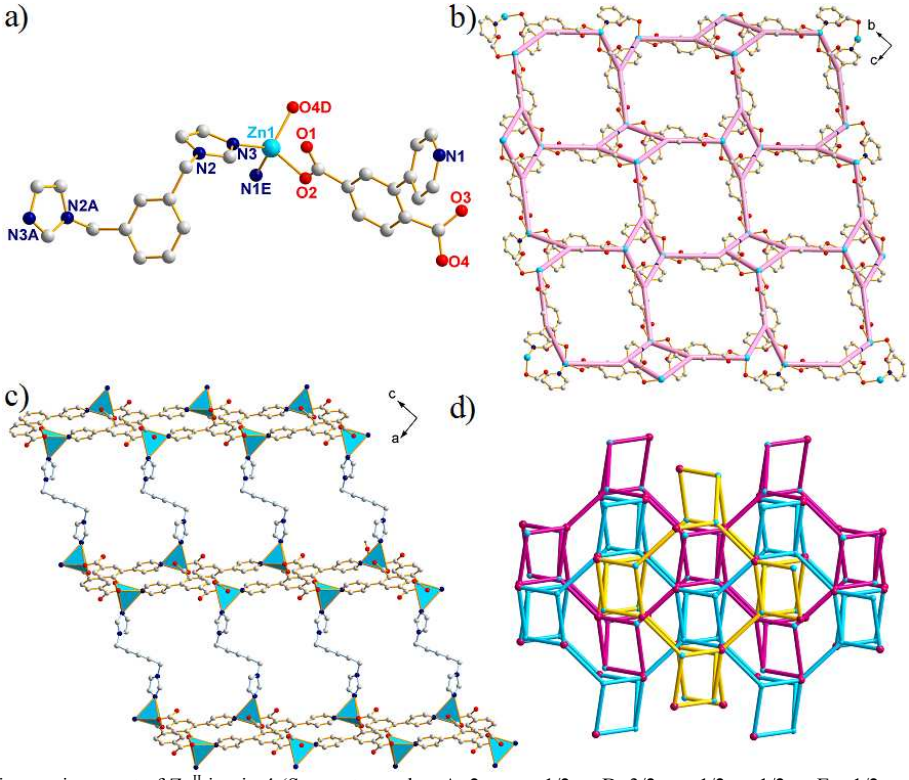

Figure 4. (a) Coordination environment of Zn^{II} ion in **4** (Symmetry codes: A: 2–*x*, *y*, –1/2–*z*; D: 3/2–*x*, –1/2+*y*, 1/2–*z*; E: –1/2+*x*, 1/2–*y*, –1/2+*z*.). (b) The 3,3-connected $[Zn(pta)]_n$ sheet along *a* axis. (c) Schematic view of the 3D structure frameworks of **4** along *b* axis. (d) The 3-fold 3D→3D parallel entangled (3,4)-connected $(4.6.8)(4.6^2.8^3)$-**3,4T1** net.

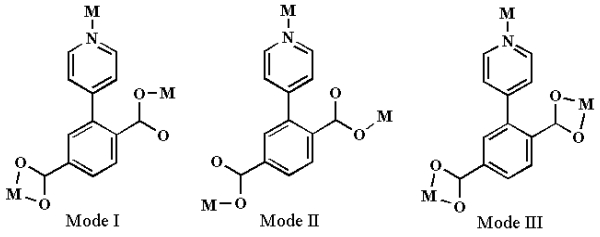

Scheme 2. The coordination modes of H_2pta in complexes **1**-**4**.

Structure descriptions of $\{[Zn(pta)(1,3\text{-bimb})_{0.5}]\cdot 1.5H_2O\}_n$ (4). Similar to complex **3**, complex **4** also owns a 3-fold 3D→3D parallel entangled (3,4)-connected networks. X-ray single-crystal diffraction analysis reveals that complex **4** crystallizes in the monoclinic system, *C2/c* space group. There are one Zn^{II} ion, one pta^{2-} ligand, half of 1,3-bimb ligand, and one and half lattice water molecules in the asymmetric unit. As shown in Fig. 4a, Zn^{II} is coordinated by two O atoms from two pta^{2-} ligands and two N atoms from two 1,3-bimb ligands, exhibiting a distorted tetrahedron geometry. The bond lengths of Zn–O are 1.972(4) and 1.980(4) Å, and the Zn–N bond lengths are 1.988(5) and 2.070(4) Å, respectively.

In complex **4**, pta^{2-} ligand exhibits the coordination mode of Mode II. The pta^{2-} ligand linked three Zn^{II} ions into a 2D 3,3-connected $[Zn(pta)]_n$ layer (Fig. 4b), which are further expanded to a 3D porous framework with 1,3-bimb linkers as pillars (Fig. 4c). Moreover, three independent frameworks are interpenetrated to form a more stable 3D networks. Different from the C–H···π interactions in complex **2**, the π-π interactions in complex **3**, containing the π-π interactions [Cg···Cg =3.775 Å] between the phenyl ring of pta^{2-} and pyridyl ring of another pta^{2-}, and the π-π interactions [Cg···Cg =3.672 Å] between two adjacent imidazol ring make the 3D interpenetrating structure more stable. The topology analysis shows that the overall framework of complex **4** can be rationalized to a 3-fold binodal (3,4)-connected **3,4T1** net with the Point Schläfli symbol of $(4.6.8)(4.6^2.8^3)$ by denoting pta^{2-} as 3-connected nodes and Zn^{II} ions as 4-connected nodes, respectively (Fig. 4d).

Structural Comparison and Discussion. As shown in the Scheme 2 and Table 2, the H_2pta ligands are completely deprotonated and exhibit three different coordination modes. All pta^{2-} ligands coordinated with three transition metal ions by using the pyrindyl N atom and monodentate/chelating carboxyl groups. Besides, all the pta^{2-} ligands holding the dihedral angle between phenyl ring and pyridyl ring, indicating the conformation of pta^{2-} ligands have adjustments when coordinating with the metal ions. For complex **1**, the pta^{2-} ligands linked Cu^{II} ions into a 3,4-connected $[Cu(pta)]_n$ sheet. And then the 1D $[Cu(1,4\text{-bimb})]_n$ chains tandemed the neighbourbing $[Cu(pta)]_n$ sheets, leaving a (3,4,4)-connected $(4.8^2)_2(4^2.8^2.10^2)(8.10^4.12)$ architecture. As for complex **2**, a 1D $[Co(pta)]_n$ ladder chain was obtained thorugh the interactions between the pta^{2-} ligands and Co^{II} ions. By sharing the Co^{II} ions with a 1D snaked $[Co(4,4'\text{-bibmp})]_n^{2n+}$, a 2D (3,5)-connected **3,5L2** sheet was constructed. Different from the 1D metal-bis(imidazole) linker chains in complex **1** and **2**, the bis(imidazole) linkers in complex **3** and **4** are just bridging the

adjacent 2D $[M(pta)]_n$ layers, constructing 3D frameworks with 1D channels. And then the 3D nets interpenetrated with each other, giving 3-fold 3,4-connected $(4.6.8)(4.6^2.6^3)$-**fsc-3,4-C2/c** net for **3**, and $(4.6.8)(4.6^2.8^3)$-**3,4T1** net for **4**. The minor difference between complex **3** and **4** can mainly attribted to the divergence of angles among organic linkers around metal ions.

Table 2 The comparisons of complexes **1**–**4**.

Complex	Coord. Mode	Ancillary Ligands/Roles/Separated M···M distance (Å)	Dihedral Angle (°) of H_2pta	Structure and Topology
1	Mode I	1,4-bimb/bridging/13.897(5)	44.53(1)	3D (3,4,4)-connected $(4.8^2)_2(4^2.8^2.10^2)(8.10^4.12)$ net
2	Mode II	4,4'-bimbp/bridging/14.637(4)	50.84(8)	2D (3,5)-connected $(4^2.6^7.8)(4^2.6)$-**3,5L2** sheet
3	Mode III	1,4-bidb/bridging/13.784(2)	49.52(0)	3-fold 3D (3,4)-connected $(4.6.8)(4.6^2.6^3)$-**fsc-3,4-C2/c** net
4	Mode II	1,3-bimb/bridging/13.119(8)	47.70(3)	3-fold 3D (3,4)-connected $(4.6.8)(4.6^2.8^3)$-**3,4T1** net

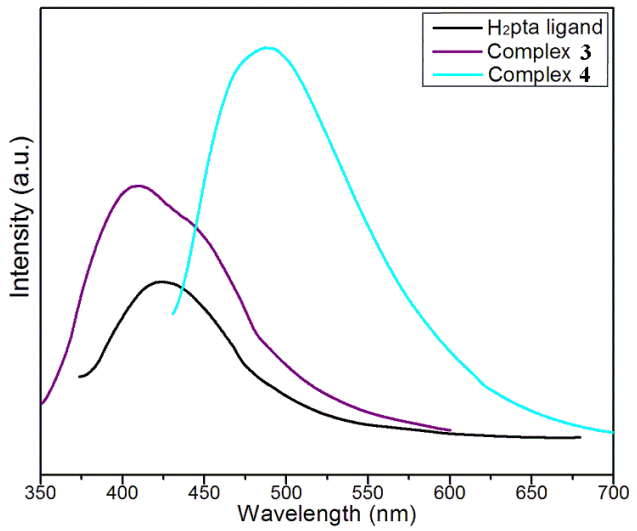

Figure 5. Emission spectra of H_2pta and complexes **3** and **4** in the solid state at room temperature.

In summary, the bis(imidazole) bridging linkers can modulate their conformations to fine-tune themselves to satisfy the coordination preference of metal centers, which often leads to structural changes and affords unprecedented architectures. The mixed−ligands synthetic strategy has advantages for their synergistic effects of two linkers.

Thermal Analyses. The experiments of thermogravimetric analysis (TGA) were performed under N_2 atmosphere with a heating rate of 10 °C min^{-1}, shown in Fig. S3. For complex **1**, the first weight loss in the temperature range of 85-135°C is consistent with the removal of the coordinated and lattice water molecules (obsd 6.5 %, calcd 6.0 %). And then the packing structure starts to collapse with the temperature increasing. For complex **2**, the framework is stable until 385°C after released the coordinated and lattice water molecules (obsd 5.1 %, calcd: 4.2 %), and then it starts to lose its organic ligands as a result of thermal decomposition with the final remaining weight is ca. 13.6 % (calcd. for Co_2O_3 12.7 %). For complex **3**, an initial weight loss of 7.5 % corresponds to the loss of lattice water molecules (calcd: 7.1 %). Above 350°C, the second weight loss corresponds to the loss of the organic ligands. The TGA curve of complex **4** displays the first loss of 6.3 % in the temperature range of 90-140°C corresponding to the loss of lattice water molecules (calcd: 5.9 %). And then the framework collapses with thermal stability residues.

Photoluminescence Properties. The fluorescence spectrum of H_2pta and complex **3**, and **4** have been investigated in the solid state at room temperature, shown in Fig. 5. The photoluminescent spectra of H_2pta show the main peaks at 423 nm under 353 nm wavelength excitation, which could be attributed to the π*→n or π*→π transitions.[17] The emission spectra exhibit emission peaks of 408 nm (λ_{ex} = 330 nm) for **3**, and 487 nm (λ_{ex} = 412 nm) for **4**, respectively, which can be assigned to the intraligand (π*→n or π*→π) emission because these emissions are neither metal-to-ligand charge transfer (MLCT) nor ligand-to-metal transfer (LMCT) in nature since the Cd^{II} and Zn^{II} ions are difficult to oxidize or reduce due to its d^{10} configuration.[18] The difference of the emission behaviours for complexes **3** and **4** probably derives from the different conformations of organic ligands and the differences in the rigidity of solid state crystal packing structures. The luminescence lifetime for complexes **3** and **4** were recorded at room temperature on an Edinburgh FLS920 phosphorimeter with a 450 W xenon lamp as excitation source. And the luminescence lifetimes of complexes **3** and **4** are 2.29 ns (for **3**) and 2.46 ns (for **4**), respectively.

Conclusions

In summary, four CPs were synthesized by employing bifunctional 6-(4-pyridyl)-terephthalic acid (H_2pta) and four different bis(imidazole) bridging linkers, which exhibiting a systematic variation of architectures from (3,4,4)-connected $(4.8^2)_2(4^2.8^2.10^2)(8.10^4.12)$ architecture, 2D (3,5)-connected **3,5L2** sheet, 3-fold (3,4)-connected **fsc-3,4-C2/c** net, to 3-fold (3,4)-connected **3,4T1** net. These results reveal that the bifunctional 6-(4-pyridyl)-terephthalic acid is a good candidate and the mixed-ligands synthetic strategy has advantages for their synergistic effects of two linkers. Moreover, the luminescence properties of complexes **3** and **4** in solid state show strong purple and green fluorescence in the solid state at room temperature, indicate that these compounds may be potential fluorescence materials.

Acknowledgements

The work was supported by financial support from the Natural Science Foundation of China (Grant Nos. 21101097, 21451001), Natural Science Foundation of Shandong Province (ZR2010BQ023), key discipline and innovation team of Qilu Normal University.

Notes

The authors declare no competing financial interest.

References

1. (a) W. Shi, S. Song and H. Zhang, *Chem. Soc. Rev.*, 2013, **42**, 5714; (b) G. Férey and C. Serre, *Chem. Soc. Rev.*, 2009, **38**, 1380; (c) B.

L. Chen, N. W. Ockwig, A. R. Millward, D. S. Contreras and O. M. Yaghi, *Angew. Chem. Int. Ed*., 2005, **44**, 4745; (d) M. Kim, J. F. Cahill, H. Fei, K. A. Prather and S. M. Cohen, *J. Am. Chem. Soc*., 2012, **134**, 18082; (e) Z. Hao, G. Yang, X. Song, M. Zhu, X. Meng, S. Zhao, S. Song and H. Zhang, *J. Mater. Chem. A*, 2014, **2**, 237; (g) M. Zhang, W. Lu, J. R. Li, M. Bosch, Y. P. Chen, T. F. Liu, Y. Liu and H. C. Zhou, *Inong. Chem. Front.*, 2014, **1**, 159; (f) D. S. Li, Y. P. Wu, J. Zhao, J. Zhang and J. Y. Lu, *Coord. Chem. Rev*., 2014, **261**, 1.

2. (a) S. Chen, R. Shang, K. L. Hu, Z. M. Wang and S. Gao, *Inong. Chem. Front.*, 2014, **1**, 83; (b) X. T. Zhang, D. Sun, B. Li, L. M. Fan, B. Li and P. H. Wei, *Cryst. Growth Des.*, 2012, **12**, 3845; (c) X. J. Kong, Y. Wu, L. S. Long, L. S. Zheng and Z. Zheng, *J. Am. Chem. Soc*., 2009, **131**, 6918; (d) Z. Hao, X. Song, M. Zhu, X. Meng, S. Zhao, S. Su, W. Yang, S. Song and H. Zhang, *J. Mater. Chem. A*, 2013, **1**, 11043; (e) W. Liu, X. Bao, L. L. Mao, J. Tucek, R. Zboril, J. L. Liu, F. S. Guo, Z. P. Ni and M. L. Tong, *Chem. Commun.*, 2014, **50**, 4059; (f) S. L. Huang, Y. J. Lin, T. S. A. Hor and G. X. Jin, *J. Am. Chem. Soc*., 2013, **135**, 8125.

3. (a) D. Sun, S. Yuan, H. Wang, H. F. Lu, S. Y. Feng and D. F. Sun, *Chem. Commun*., 2013, **49**, 6152; (b) X. Zhang, L. Fan, W. Zhang, Y. Ding, W. Fan and X. Zhao, *Dalton Trans.,* 2013, **42**, 16562; (c) J. B. Lin, W. Xue, B. Y. Wang, J. Tao, W. X. Zhang, J. P. Zhang and X. M. Chen, *Inorg. Chem*., 2012, **51**, 9423; (d) K. Wang, S. Zeng, H. Wang, J. Dou and J. Jiang, *Inong. Chem. Front.*, 2014, **1**, 167; (e) L. Fan, W. Fan, W. Song, G. Liu, X. Zhang and X. Zhao, *CrystEngComm*, 2014, **16**, 9191; (f) J. L. Liu, Y. C. Chen, Y. Z. Zheng, W. Q. Lin, L. Ungur, W. Wernsdorfer, L. F. Chibotaru and M. L. Tong, *Chem. Sci*., 2013, **4**, 3310.

4. (a) L. Li, J. Ma, C. Song, T. Chen, Z. Sun, S. Wang, J. Luo and M. Hong, *Inorg. Chem.*, 2012, **51**, 2438; (b) C. C. Ji, J. Li, Y. Z. Li, Z. J. Guo and H. G. Zheng, *CrystEngComm.,* 2011, **13**, 459; (c) D. Sun, L. L. Han, S. Yuan, Y. K. Deng, M. Z. Xu and D. F. Sun, *Cryst. Growth Des.*, 2013, **13**, 377; (d) X. H. Chang, J. H. Qin, M. L. Han, L. F. Ma and L. Y. Han, *CrystEngComm*, 2014, **16**, 870; (e) L. Liu, C. Yu, J. Sun, P. Meng, F. Ma, J. Du and L. Ma, *Dalton Trans.,* 20134, **43**, 2915; (f) Q. L, Zhang, G. W. Feng, Y. Q. Zhang and B. X. Zhu, *RSC Advances*, 2014, **4**, 11384.

5. (a) S. Chen, R. Shang, K. L. Hu, Z. M. Wang and S. Gao, *Inong. Chem. Front*., 2014, **1**, 83; (b) L. Fan, X. Zhang, D. Li, D. Sun, W. Zhang and J. Dou, *CrystEngComm*, 2013, **15**, 349; (c) H. Zhou, G. X. Liu, X. F. Wang and Y. Wang, *CrystEngComm.*, 2013, **15**, 1377; (d) S. Song, X. Song, S. Zhao, C. Qin, S. Su, M. Zhu, Z. Hao and H. Zhang, *Dalton. Trans*., 2012, **41**, 10412; (e) G. L. Liu and H. Liu, *CrystEngComm*, 2013, **15**, 6870; (f) C. Zhan, C. Zou, G. Q. Kong and C. D. Wu, *Cryst. Growth Des.*, 2013, **13**, 1429.

6. (a) C. Zhang, H. Hao, Z. Shi and H. Zheng, *CrystEngComm*, 2014, **16**, 5662; (b) N. Zhang, Y. Tai, M. Liu, P. Ma, J. Zhao and J. Niu, *Dalton Trans.,* 2014, **43**, 5182; (c) W. Meng, Z. Xu, J. Ding, D. Wu, X. Han, H. Hou and Y. Fan, *Cryst. Growth Des.*, 2014, **14**, 730; (d) (e) D. W. Tan, J. B. Xie, Q. Li, H. X. Li, J. C. Li, H. Y. Li and J. P. Lang, *Dalton Trans.,* 2014, **43**, 14061; (f) M. L. Han, X. H. Chang, X. Feng, L. F. Ma and L. Y. Wang, *CrystEngComm.*, 2014, **16**, 1687.

7. (a) F. Meng, L. Qin, M. Zhang and H. Zheng, *CrystEngComm*, 2014, **16**, 698; (b) M. L. Han, Y. P. Duan, D. S. Li, H. B. Wang, J. Zhao and Y. Y. Wang, *Dalton Trans.,* 2014, **43**, 15450; (c) Y. B. Wang, Y. L. Lei, S. H. Chi and Y. J. Luo, *Dalton Trans.,* 2013, **42**, 1862; (d) B. Liu, D. S. Li, L. Hou, G. P. Yang, Y. Y. Wang and Q. Z. Shi, *Dalton Trans.,* 2013, **42**, 9822; (e) X. T. Zhang, L. M. Fan, X. Zhao, D. Sun, D. C. Li and J. M. Dou, *CrystEngComm*, 2012, **14**, 2053; (f) X. Zhang, L. Fan, Z. Sun, W. Zhang, W. Fan, L. Sun and X. Zhao, *CrystEngComm*, 2013, **15**, 4910; (g) J. Zhao, L. Q. Xie, Y. M. Ma, A. J. Zhou, W. Dong, J. Wang, Y. C. Chen and M. L. Tong, *CrystEngComm*, 2014, **16**, 10006.

8. (a) Y. M. Klein, E. C. Constable, C. E. Housecroft, J. A. Zampese and A. Crochet, *CrystEngComm*, 2014, **16**, 9915; (b) X. H. Chang, Y. Zhao, M. L. Han, L. F. Ma and L. Y. Wang, *CrystEngComm*, 2014, **16**, 6417; (c) E. C. Constable, C. E. Housecroft, A. Prescimone, S. Vujovic and A. Crochet, *CrystEngComm*, 2014, **16**, 8691.

9. (a) F. L. Hu, Y. Mi, Y. Q. Gu, L. G. Zhu, S. L. Yan, H. Wei and J. P. Lang, *CrystEngComm*, 2013, **15**, 9553; (b) X. T. Zhang, L. M. Fan, W. Zhang, Y. S. Ding, W. L. Fan, L. M. Sun, X. Zhao and H. Lei, *Cryst. Growth Des*., 2013, **13**, 2462; (c) Y. G. Sun, J. Li, K. L. Li, Z. H. Xu, F. Ding, B. Y. Ren, S. J. Wang, L. X. You, G. Xiong and P. F. Smet, *CrystEngComm*, 2014, **16**, 1777; (d) J. P. Zhao, Q. Yang, S. D. Han, J. Han, R. Zhao, B. W. Hu and X. H. Bu, *Dalton Trans.,* 2013, **42**, 8201.

10. (a) L. L. Liu, C. X. Li, J. Sun, P. P. Meng, F. J. Ma, J. M. Du and J. F. Ma, *Dalton Trans.,* 2014, **43**, 2915; (b) H. Li, Y. Han, X. Lv, S. Du, H. Hou and Y. Fan, *CrystEngComm*, 2013, **15**, 3672; (c) J. Huang, H. Li, J. Zhang, L. Jiang, C. Y. Su, *Inorg. Chem. Comm.*, 2012, **388**, 16; (d) S. J. Liu, L. Xue, T. L. Hu and X. H. Bu, *Dalton Trans.,* 2012, **41**, 6813; (e) J. Y. Lu, *Coord. Chem. Rev*., 2003, **246**, 327.

11. (a) F. Guo, B. Zhu, M. Liu, X. Zhang, J. Zhang and J. Zhao, *CrystEngComm*, 2013, **15**, 6191; (b) L. Fan, X. Zhang, W. Zhang, Y. Ding, W. Fan, L. Sun, Y. Pang and X. Zhao, *Dalton Trans.,* 2014, **43**, 6701; (c) X. Zhang, L. Fan, W. Zhang, W. Fan, L. Sun and X. Zhao, *CrystEngComm*, 2014, **16**, 3203; (d) B. Liu, L. Wei, N. N. Li, W. P. Wu, H. Miao, Y. Y. Wang and Q. Z. Shi, *Cryst. Growth Des*., 2014, **14**, 1110; (e) X. H. Chang, J. H. Qin, M. L. Han, L. F. Ma, L. Y. Wang, *CrystEngComm*, 2014, **16**, 870.

12. (a) S. Wang, Y. Peng, X. Wei, Q. Zhang, D. Wang, J. Dou, D. Li and J. Bai, *CrystEngComm*, 2011, **13**, 5313; (b) B. Ji, D. Deng, L. Ma, H. Li, X. Fan, G. Ou, L. Cao and L. Zhou, *CrystEngComm*, 2013, **15**, 4107; (c) J. H. Qin, L. F. Ma, Y. Han and L. Y. Wang, *CrystEngComm*, 2012, **14**, 2891; (d) L. F. Ma, J. W. Zhao, M. L. Han, L. Y. Wang and M. Du, *Dalton Trans.,* 2012, **41**, 2078; (e) X. Zhang, L. Fan, W. Song, W. Fan, L. Sun and X. Zhao, *RSC Adv.*, 2014, **4**, 30274; (f) L. Fan, W. Fan, B. Li, X. Liu, X. Zhao and X. Zhang, *Dalton. Trans*., 2014, **DOI:** 10.1039/C4DT03076A.

13. (a) Y. W. Li, D. C. Li, J. Xu, H. G. Hao, S. N. Wang, J. M. Dou, T. L. Hu and X. H. Bu, *Dalton. Trans*., 2012, **41**, 15708; (b) L. Fan, Y. Gao, G. Liu, W. Fan, W. Song, L. Sun, X. Zhao and X. Zhang, *CrystEngComm*, 2014, **16**, 7649; (c) L. Fan, W. Fan, W. Song, L. Sun, X. Zhao and X. Zhang, *Dalton. Trans*., 2014, **43**, 15979; (d) Z. H. Yan, L. L. Han, Y. Q. Zhao, X. Y. Li, X. P. Wang, L. Wang and D. Sun, *CrystEngComm*, 2014, **16**, 8747; (e) X. Zhao, T. Wu, X. Bu and P. Feng, *Dalton. Trans*., 2011, **40**, 8072.

14. (a) G. M. Sheldrick, *SHELXTL*, version 5.1; Bruker Analytical X-ray Instruments Inc.: Madison, WI, 1998. (b) G. M. Sheldrick, *SHELX-97*, PC Version; University of Gottingen: Gottingen, Germany, 1997.

15. (a) L. Fan, X. Zhang, W. Zhang, Y. Ding, W. Fan, L. Sun and X. Zhao, *CrystEngComm*, 2014, **16**, 2144; (b) L. L. Liu, C. X. Yu, Y. Zhou, J. Sun, P. P. Meng, D. Liu and R. J. Sa, *Inorg. Chem. Commun*, 2014, **40**, 194; (c) X. T. Zhang, L. M. Fan, Z. Sun, W. Zhang, D. C. Li, J. M. Dou and L. Han, *Cryst. Growth Des*., 2013, **13**, 792.

16. (a) V. A. Blatov, A. P. Shevchenko and V. N. Serezhkin, *J. Appl. Crystallogr.*, 2000, **33**, 1193; (b) The network topology was evaluated by the program "TOPOS-4.0", see: http://www.topos.ssu.samara.ru. (c) V. A. Blatov, M. O'Keeffe and D. M. Proserpio, *CrystEngComm*, 2010, **12**, 44.

17. (a) T. Liu, S. Wang, J. Lu, J. Dou, M. Niu, D. Li and J. Bai, *CrystEngComm.,* 2013, **15**, 5476; (b) L. P. Xue, X. H. Chang, S. H. Li, L. F. Ma and L. Y. Wang, *Dalton Trans.,* 2014, **43**, 7219; (c) M. L. Han, J. G. Wang, L. F. Ma, H. Guo and L. Y. Wang, *CrystEngComm*, 2012, **14**, 2691; (d) S. Yuan, Y. K. Deng, W. M. Xuan, X. P. Wang, S. N. Wang, J. M. Dou and D. Sun, *CrystEngComm*, 2014, **16**, 3829; (e) D. Sun, M. Z. Xu, S. S. Liu, S. Yuan, H. F. Lu, S. Y. Feng and D. F. Sun, *Dalton Trans.,* 2013, **42**, 12324; (f) J. Pan, F. Jiang, M. Wu, L. Chen, J. Qian, K. Su, X. Wan and M. Hong, *CrystEngComm*, 2014, **16**, 11078.

18. (a) X. F. Zhang, W. C. Song, Q. Yang and X. H. Bu, *Dalton Trans.,* 2012, **41**, 4217; (b) J. J. Wang, T. L. Hu and X. H. Bu, *CrystEngComm*, 2011, **13**, 5152; (c) D. Sun, Z. H. Yan, Y. K. Deng, S. Yuan, L. Wang and D. F. Sun, *CrystEngComm*, 2012, **14**, 7859; (d) Q. Lin, T. Wu, X. Bu and P. Feng, *Dalton. Trans*., 2012, **41**, 3620; (e) Z. H. Yan, X. W. Zhang, H. Pang, Y. Zhang, D. Sun and

L. Wang, *RSC Advances*, 2014, **4**, 53608; (f) H. Guo, Y. Yan, X. Guo, H. Zou, Y. Qi and C. Liu, *CrystEngComm.*, 2014, **16**, 10245.

RSC Advances

For Table of Contents Use Only

Table of Contents Graphic and Synopsis

Syntheses, Structures, Topologies, and Luminescence Properties of Four Coordination Polymers Based on Bifunctional 6-(4-pyridyl)-terephthalic Acid and Bis(imidazole) Bridging Linkers

Liming Fan, Weiliu Fan, Bin Li, Xinzheng Liu, Xian Zhao and Xiutang Zhang

Four CPs were synthesized by employing bifunctional 6-(4-pyridyl)-terephthalic acid (H_2pta) and four different bis(imidazole) bridging linkers through the mixed-ligand strategy, which exhibiting a systematic variation of architectures from 2D sheet to 3-fold penetrating net.